HHS Public Access

Author manuscript

*Cancer Res*. Author manuscript; available in PMC 2020 March 01.

Published in final edited form as:

*Cancer Res*. 2019 March 01; 79(5): 954–969. doi:10.1158/0008-5472.CAN-18-1790.

# Pleiotropic effects of PPARD accelerate colorectal tumorigenesis, progression, and invasion

**Yi Liu**[#1], **Yasunori Deguchi**[#1], **Rui Tian**[#1,6], **Daoyan Wei**[2], **Ling Wu**[1], **Weidong Chen**[1], **Weiguo Xu**[1], **Min Xu**[1], **Fuyao Liu**[1], **Shen Gao**[1], **Jonathan C. Jaoude**[1], **Sarah P. Chrieki**[1], **Micheline J. Moussalli**[3], **Mihai Gagea**[4], **Jeffrey Morris**[5], **Russell R. Broaddus**[3], **Xiangsheng Zuo**[1,7], and **Imad Shureiqi**[1,7]

[1]Department of Gastrointestinal Medical Oncology, The University of Texas MD Anderson Cancer Center, Houston, Texas 77030, USA

[2]Department of Gastroenterology, Hepatology, and Nutrition, The University of Texas MD Anderson Cancer Center, Houston, Texas 77030, USA

[3]Department of Pathology, The University of Texas MD Anderson Cancer Center, Houston, Texas 77030, USA

[4]Department of Veterinary Medicine & Surgery, The University of Texas MD Anderson Cancer Center, Houston, Texas 77030, USA

[5]Department of Biostatistics, The University of Texas MD Anderson Cancer Center, Houston, Texas 77030, USA

[6]Department of Biliary-Pancreatic Surgery, Affiliated Tongji Hospital, Tongji Medical College, Huazhong University of Science and Technology, Wuhan, Hubei, 430030, China.

[#] These authors contributed equally to this work.

## Abstract

APC mutations activate aberrant β-catenin signaling to drive initiation of colorectal cancer (CRC), however, CRC progression requires additional molecular mechanisms. PPAR-delta (PPARD), a downstream target of β-catenin, is upregulated in CRC. However, promotion of intestinal tumorigenesis following deletion of PPARD in $Apc^{min}$ mice has raised questions about the effects of PPARD on aberrant β-catenin activation and CRC. In this study, we used mouse models of PPARD overexpression or deletion combined with APC mutation ($Apc^{\Delta 580}$) in intestinal epithelial cells (IEC) to elucidate the contributions of PPARD in CRC. Overexpression or deletion of

[7]**Correspondence to**: Imad Shureiqi or Xiangsheng Zuo, Department of Gastrointestinal Medical Oncology, The University of Texas MD Anderson Cancer Center, 1515 Holcombe Boulevard, Houston, TX 77030-4009. Phone: (713) 792-2828; ishureiqi@mdanderson.org or xzuo@mdanderson.org.

AUTHOR CONTRIBUTIONS

I.S. developed the conceptual framework. I.S., X.Z., and Y.L. designed the experiments and wrote the manuscript. X.Z., Y.L, Y.D., R.T., L.W., W.C., W.X., M.X., F.L., S.G., J.C.J., S.P.C, and M.J.M performed experiments. X.Z., Y.L, Y.D., and I.S. analyzed the data. J.M. supervised and contributed to the statistical analyses. Y.D., M.G., and R.B. performed pathology analyses. D.W. provided conceptual feedback on the manuscript.

SUPPLEMENTAL INFORMATION

Supplemental information includes supplementary methods, 7 supplementary figures and 2 supplementary tables and can be found with this article online.

**Declaration of conflict of interest:** The authors declare no competing interests

PPARD in IEC augmented or suppressed β-catenin activation via up- or downregulation of BMP7/TAK1 signaling and strongly promoted or suppressed CRC, respectively. Depletion of PPARD in human CRC organoid cells inhibited BMP7/β-catenin signaling and suppressed organoid self-renewal. Treatment with PPARD agonist GW501516 enhanced CRC tumorigenesis in $Apc^{\Delta 580}$ mice, whereas treatment with PPARD antagonist GSK3787 suppressed tumorigenesis. PPARD expression was significantly higher in human CRC invasive fronts versus their paired tumor centers and adenomas. Reverse-phase protein microarray and validation studies identified PPARD-mediated upregulation of other pro-invasive pathways: connexin 43, PDGFRβ, AKT1, EIF4G1, and CDK1. Our data demonstrate that PPARD strongly potentiates multiple tumorigenic pathways to promote CRC progression and invasiveness.

**Keywords**

PPAR-delta; Beta-catenin; colorectal cancer; invasion; PDGFRβ

## INTRODUCTION

APC mutations activate aberrant β-catenin signaling to drive colorectal tumorigenesis (1). However, colorectal cancer (CRC) progression, especially invasiveness, requires additional molecular mechanisms (2,3). The presence of CRC invasion in colorectal polyps profoundly worsen patients' outcomes (4). Identification of critical invasiveness-regulating mechanisms can therefore open a door for molecular targeting of crucial genes for CRC treatment.

The ligand-activated nuclear receptor peroxisome proliferator-activated receptor-δ/β (PPARD) has pleiotropic effects on cell homeostasis (5). PPARD is upregulated in human colorectal polyps and CRCs (6-8) and has been identified as a downstream target of the β-catenin/TCF4 complex in CRC cell lines (6). However, this proposed mechanistic link between β-catenin and PPARD has been questioned on the basis of *in vitro* and *in vivo* data (9). More importantly, germline PPARD knockout (KO) in $Apc^{min}$ mice produced conflicting results, both increasing (10) and decreasing (11) intestinal tumorigenesis. Recently, a high-fat diet was reported to increase β-catenin activation via PPARD in progenitor intestinal cells of $Apc^{min}$ mice (12). Nevertheless, the role of PPARD in colorectal tumorigenesis, especially in relation to APC and aberrant β-catenin activation, remains highly controversial (13). Filling this knowledge gap is important because PPARD is a druggable protein for which agonists and antagonists have been developed. Although the clinical testing and pharmaceutical development of PPARD agonists by large pharmaceutical companies to treat noncancerous conditions (e.g., obesity) has been halted in many instances, these agents (e.g., cardarine [GW501516]) are still sold on the internet black market to individuals such as athletes wishing to enhance muscle endurance. Therefore, preclinical data clarifying the role of PPARD in CRC are urgently needed to educate the public about the potential risk of promoting CRC with PPARD agonists.

We therefore tested PPARD's effects on aberrant β-catenin activation-driven colon tumorigenesis using murine genetic models of human CRC with representative APC mutations (14) with concomitant PPARD overexpression or deletion in intestinal epithelial

cells (IECs). Our data showed that PPARD strongly enhanced aberrant β-catenin activation and more importantly it robustly activated multiple pro-invasive pathways to promote CRC tumorigenesis.

## MATERIALS AND METHODS

### Cell lines

Cell lines were grown as described previously (8). SW480, SW620, and CT26 cells were purchased from ATCC; and HCT116 wild-type and HCT116 with PPARD genetic KO (KO1) cells were kindly provided by Dr. Bert Vogelstein. The cell lines were authenticated by short tandem repeat analyses, and mycoplasma was routinely tested.

### Human tissue materials

Human colorectal tissue samples were collected after obtaining written informed consent from the patients. The current studies using these tissue samples were conducted in accordance with the recognized ethical guidelines (Declaration of Helsinki, CIOMS, Belmont Report, and U.S. Common Rule) and approved by the University of Texas MD Anderson Cancer Center Institutional Review Board. De-identified sections from paraffin-embedded tissue blocks of archived surgical pathology materials were obtained from the colorectal tumor tissue repository at the University of Texas MD Anderson Cancer Center. These sections from 41 CRC patients, who underwent surgical resection of CRC without prior exposure to chemotherapy or radiation therapy, contained areas of adenomatous polyps and cancer arising within the polyps and paired normal-appearing colonic mucosa in the same hematoxylin and eosin (H&E)-stained section for each case, confirmed by an experienced colon pathologist (R.B.).

De-identified fresh CRC tissues were obtained from patients undergoing surgical resection of CRC at MD Anderson Cancer Center to derive CRC organoids. RNA samples from paired normal and malignant colonic mucosa from patients with stage III colon cancer were obtained from MD Anderson Cancer Center as described previously (8).

### Mouse models

Mouse care and experimental protocols were approved and conducted in accordance with the guidelines of the Animal Care and Use Committee of The University of Texas MD Anderson Cancer Center. We generated the mice with targeted PPARD overexpression in IECs via a villin promoter (designated as PD mice) as described previously (15). C57BL/6J-*Apc*$^{Min}$/J (Apc$^{min}$, stock #002020), B6.Cg-Tg (CDX2-Cre) 101Erf/J (CDX2-Cre, stock # 009350), and B6.Cg-Tg (CDX2-Cre/ERT2)752Erf/J (CDX2-CreERT2, stock #022390) mice were purchased from Jackson Laboratory. Apc$^{\Delta 580}$-flox mice, in which APC exon 14 is flanked with *loxP* sites, were a gift from Dr. Kenneth E. Hung (16). PPARD-flox mice, in which PPARD exon 4 is flanked with *loxP* sites (designated as PD-flox mice), were a gift from Dr. Ronald Evans (17). Breeding of Apc$^{\Delta 580}$-flox mice with Cre recombinase-expressing mice (CDX2-cre or CDX2-CreERT2) deleted APC exon 14 and consequently generated a codon 580 frame-shift mutation without (Apc$^{\Delta 580}$-flox;CDX2-Cre, designated

as $Apc^{\Delta 580}$ mice) or with tamoxifen treatment ($Apc^{\Delta 580}$-flox;CDX2-CreERT2, designated as $Apc^{\Delta 580\text{-}TMX}$ mice).

## Mouse intestinal tumorigenesis evaluation and survival experiments

1) $Apc^{min}$ mice were bred with PD mice to generate $Apc^{min}$-PD mice. $Apc^{min}$ and $Apc^{min}$-PD mice were followed to the age of 8 weeks. 2) $Apc^{\Delta 580}$ mice were bred with PD mice to generate $Apc^{\Delta 580}$-PD. $Apc^{\Delta 580}$ and $Apc^{\Delta 580}$-PD mice were followed until the age of either 14 weeks or 20 weeks. 3) $Apc^{\Delta 580}$ mice at age 4 weeks were fed a diet containing 50 mg/kg GW501516 or the same diet without GW501516 (control diet) (Envigo) for 10 consecutive weeks. The chemical GW501516 was synthesized by the Translational Chemistry Core Facility at MD Anderson Cancer Center, and its authenticity was confirmed by liquid chromatography-mass spectrometry (LC-MS) using standard GW501516 (Sigma). 4) $Apc^{\Delta 580\text{-}TMX}$ mice were bred with PD mice to generate $Apc^{\Delta 580\text{-}TMX}$-PD mice. $Apc^{\Delta 580\text{-}TMX}$ and $Apc^{\Delta 580\text{-}TMX}$-PD mice were treated with tamoxifen (Sigma) dissolved in corn oil (0.75 mg/10 g mice) by gavage once a day for 3 consecutive days and then followed for up to 55 weeks. 5) $Apc^{\Delta 580}$ mice were bred with PPARD-flox mice to generate PPARD knockout (KO) via deletion of PPARD's exon 4 in $Apc^{\Delta 580}$ mice, designated as $Apc^{\Delta 580}$-PD-KO mice. $Apc^{\Delta 580}$ and $Apc^{\Delta 580}$-PD-KO mice were followed until the age of 14 weeks. 6) $Apc^{\Delta 580}$ mice at age 4 weeks were fed a diet containing 200 mg/kg GSK3787 or the same diet without GSK3787 (control diet) (Envigo) for 12 consecutive weeks. GSK3787 was synthesized by the Applied Cancer Science Institute at MD Anderson Cancer Center, and its authenticity was confirmed by LC-MS analyses using standard GSK3787 (Sigma).

The mice were euthanized, and the intestines from the rectum to the base of the stomach were removed, opened, washed with phosphate-buffered saline and fixed with 10% neutral formalin overnight. Tumors were counted under a stereotype microscope (Nikon SMZ1000). The intestines were rolled up using a paper clip with a small loop to make Swiss rolls. The rolls were cut in half, and placed in a paraffin cassette for embedding in paraffin for further analysis. Classification and grading of H&E-stained sections, including scoring tumor invasiveness, were performed by an experienced pathologist (R.B).

Survival experiments were performed for the following groups: 1) $Apc^{\Delta 580}$ and $Apc^{\Delta 580}$-PD mice; and 2) $Apc^{\Delta 580}$ mice on a diet containing 50 mg/kg GW501516 or a control diet. For each experiment, mice were followed until they required euthanasia on the basis of 1 of the following preset criteria: (1) persistent rectal bleeding for 3 consecutive days or/and (2) weight loss of more than 20%.

## Intestine organoid culture and organoid cell viability assay

Mouse intestines and human CRC tissues were harvested and digested for 3-dimensional (3-D) organoid culture using the method as described by Clevers and colleagues (18). On day 7 of culture, mouse intestinal organoids were imaged, counted, and quantified for organoid cell viability by using CellTiter-Glo Luminescent Cell Viability Assay (Promega) according to the manufacturer's protocol.

Human CRC organoids were passaged at least 3 generations and then digested into single cells with TrypLE (Thermo Scientific) and plated in 24-well plates with the Ultra-Low

Attachment surface (Corning). The cells were then transfected with 30 nM of ON-TARGETplus PPARD small interfering RNA (siRNA) SMARTpool (Dharmacon) or a nonspecific control siRNA (Dharmacon) using Lipofectamine RNAiMAX (Invitrogen). Forty-eight hours after transfection, cells were harvested for RNA measurement. In addition, the organoid cells were seeded with Matrigel for 3-D organoid culture 24 hours after siRNA transfection. Seventy-two hours after the cells were with Matrigel, organoid cell viability was measured as described above.

### Western blotting and functional proteomics reverse-phase protein array analysis

Western blotting was performed as described before (8). Reverse-phase protein array (RPPA) analysis was performed on isolated IECs from $Apc^{\Delta 580}$ mice and their $Apc^{\Delta 580}$-PD littermates according to the standard protocol at the RPPA Core Facility at MD Anderson (19). Information about the RPPA antibodies is available at https://www.mdanderson.org/research/research-resources/core-facilities/functional-proteomics-rppa-core/antibody-information-and-protocols.html.

### Statistical analyses

Quantifiable outcome measures for 1 factor in experimental conditions were compared using unpaired Student *t*-test or 1-way analysis of variance, and Bonferroni adjustments were used for all multiple comparisons. We used 2-way analysis of variance to analyze data involving the simultaneous consideration of 2 factors. Tumor incidence was compared using chi-square tests. Survival rates as a function of time were estimated using the Kaplan-Meier method. The data were log-transformed as necessary to accommodate the normality and homoscedasticity assumptions implicit to the statistical procedures used. Data were analyzed using SAS software, version 9.4 (SAS Institute, Cary, NC) or GraphPad Prism 7.01. All tests were 2 sided and conducted at a significance level of $P < 0.05$.

Additional experimental method details are included in the online Supplemental Methods section.

## RESULTS

### PPARD enhances β-catenin activation in IECs

Aberrant β-catenin activation via APC mutations upregulates PPARD (6). We therefore tested whether PPARD upregulation is sufficient to increase β-catenin activation independently of APC mutations by using PD mice with WT APC (Fig. S1A). PPARD overexpression markedly increased active β-catenin protein levels (Fig. 1A) and mRNA levels of Axin2 and cyclinD1, downstream targets of active β-catenin, in IECs (Fig. 1B). The PPARD agonist GW501516 augmented β-catenin activation by PPARD in PD mice (Fig. S1B). Aberrant β-catenin activation expands the dedifferentiated intestinal stem cell population to promote colorectal tumorigenesis (20). Intestinal organoid formation, especially primitive spheroids, was significantly higher when derived from PD mice than WT-littermates (Fig. 1C; Fig. S1C).

We examined whether PPARD activates β-catenin independently of APC mutations in HCT116 human CRC cells, which have WT APC but a heterozygous β-catenin-activating mutation (1) and found that PPARD knock-out (KO1) significantly decreased active β-catenin expression (Fig. 1D), transcriptional activity (Fig. 1E), and target gene expression (Axin2, cyclin D1, and c-Myc) (Fig. 1F). PPARD overexpression in HCT116 cells increased active β-catenin protein levels (Fig. 1G). GW501516 significantly increased active β-catenin protein levels with and without Wnt3a in HCT116 cells (Fig. S1D). Another PPARD agonist, GW0742, increased c-Myc mRNA expression in HCT116 parental cells (WT) but not in KO1 cells, whereas the PPARD antagonist GSK3787 decreased c-Myc mRNA expression even in GW0742-treated cells (Fig. S1E). GW0742 increased while GSK3787 decreased angiopoietin-like 4 (AngPTL4), a PPARD target gene, expression in HCT116 cells (Fig. S1F). PPARD downregulation by siRNA in primary human CRC organoids (Fig. S1G) decreased active β-catenin, Axin-2, c-Myc, and cyclin D1 levels and organoid regeneration (Fig. 1H-J).

$Apc^{min}$ mice mainly develop small intestinal adenomas, unlike humans, in whom intestinal tumorigenesis is essentially colorectal and can progress to invasive cancer. However, APC mutation targeting into the intestines via CDX2 promoter-driven Cre recombinase expression to produce a codon 580 frame-shift mutation ($Apc^{\Delta 580}$ mice) induces CRCs (14). $Apc^{\Delta 580}$-PD mice generated by breeding $Apc^{\Delta 580}$ with PD mice (Fig. S1H) had significantly higher PPARD (Fig. S1I), active β-catenin, Axin-2, c-Myc, and cyclin D1 levels (Fig. 1K-M) in IECs than did $Apc^{\Delta 580}$ mice. GW501516 also significantly increased active β-catenin levels in $Apc^{\Delta 580}$ mice's IECs (Fig. 1N). PPARD KO in IECs of $Apc^{\Delta 580}$ mice decreased active β-catenin and cyclin D1 levels (Fig 1O, Fig. S1J). Colonic crypt proliferative zones length significantly increased in $Apc^{\Delta 580}$-PD mice and GW501516-treated $Apc^{\Delta 580}$ mice but decreased in $Apc^{\Delta 580}$-PD-KO mice (Fig. S1K and L).

## PPARD accelerates APC mutation-driven intestinal tumorigenesis

PPARD overexpression in IECs of $Apc^{min}$ mice ($Apc^{min}$-PD mice) (Fig. S2A) rapidly and markedly increased intestinal tumor burden requiring mice euthanasia by 8 week of age (Fig. 2A and B). $Apc^{\Delta 580}$-PD mice had also significantly large intestinal tumor burden (Fig. 2C and D; Fig. S2B and C), shorter colonic lengths (Fig. S2D), and lower body weights (Fig. S2E) than did $Apc^{\Delta 580}$ mice. In longitudinal survival experiments, $Apc^{\Delta 580}$ mice survived longer (mean = 191 days) than did $Apc^{\Delta 580}$-PD mice (mean = 99 days) (Fig. 2E). Dietary GW501516 treatment of $Apc^{\Delta 580}$ mice produced significantly more and larger intestinal tumors (Fig. 2F and G; Fig. S2F and G) and shorter survival (mean = 140 days) than that of $Apc^{\Delta 580}$ mice fed a control diet (mean = 191 days) (Fig. 2H).

We further examined the effects of PPARD overexpression on adult-onset APC mutation-driven tumorigenesis using tamoxifen-inducible $Apc^{\Delta 580}$ ($Apc^{\Delta 580\text{-}TMX}$) mice to simulate the most common form of human CRC (i.e., sporadic) with an adult-onset APC mutation (Fig. S2A). $Apc^{\Delta 580\text{-}TMX}$ mice with heterozygote APC mutations induced with tamoxifen at 6 weeks of age had no visible intestinal tumors, even after 55 weeks of follow-up (only 1 small adenoma was detected microscopically). In contrast, $Apc^{\Delta 580\text{-}TMX}$-PD developed visible tumors, including large CRCs ($P = 0.025$) (Fig. 2I and J; Fig. S2H).

In contrast, PPARD KO in IECs of $Apc^{\Delta 580}$ mice (Fig. S2A), or feeding $Apc^{\Delta 580}$ mice with a PPARD antagonist (GSK3787) containing diet significantly reduced colonic tumor numbers and sizes especially the numbers of tumors larger than 3 mm (Fig. 2K-N).

## PPARD activates β-catenin via BMP7/TAK1 signaling in IECs

We screened for the molecular mechanisms by which PPARD enhanced β-catenin activation using comparative transcriptome profile analyses (RNA-seq) of HCT116 WT and KO1 cells (8) (GSE89729), and identified BMP7 mRNA expression 11-fold higher in WT cells than in KO1 cells (Fig. S3A). Independent qRT-PCR measurements confirmed this finding (Fig. 3A). BMP7 activates β-catenin by phosphorylating mitogen-activated protein kinase kinase kinase 7 (TAK1) (21). BMP7 and phosphorylated TAK1 (p-TAK1) protein levels were lower in KO1 cells than in HCT116 WT, but higher in HCT116 cells with PPARD overexpression (DDK-PPARD-HCT116) than in control vector-transfected cells (Ctrl-HCT116) (Fig. 3B). PPARD overexpression in SW480 human CRC cells with low BMP7 expression significantly increased expression of BMP7 mRNA (Fig. 3C), BMP7 protein, p-TAK1, phosphorylated P38 (p-p38), and active β-catenin protein (Fig. 3D). We next examined whether PPARD transcriptionally regulates BMP7 expression via binding to a potential PPARD binding site (pPDBS) in the BMP7 promoter, identified near the transcription start site by an in silico search using Genomatix MatInspector online software (Fig. 3E). PPARD overexpression in SW480 cells significantly increased PPARD binding to this pPDBS in the BMP7 promoter (Fig. 3F). In human CRC organoid cells, PPARD downregulation by siRNA decreased BMP7 mRNA levels (Fig. 3G).

To examine PPARD's mechanistic significance to the BMP7-TAK1-β-catenin signaling pathway, we employed a TAK1-specific inhibitor, 5z-7, to treat SW480 cells in which this signaling pathway was activated by PPARD overexpression. 5z-7 inhibited the increased active β-catenin levels by PPARD overexpression in SW480 cells (Fig. 3H). In SW620 cells with intrinsic activation of BMP7-TAK1-β-catenin signaling (21), GSK3787 reduced active β-catenin levels to those achieved with 5z-7 (Fig. 3I). In i*n vivo* studies, PPARD increased BMP7 mRNA (Fig. 3J) and BMP7, p-TAK1, p38 and active β-catenin protein levels in IECs of PD mice (Fig. 3K; Fig. S3B and C). PPARD also increased BMP7, p-TAK1, and active β-catenin protein levels in IECs of $Apc^{min}$ mice (Fig. 3L and M; Fig. S3D). Similarly, BMP7 mRNA (Fig. 3N) and BMP7, p-TAK1, p38, p-p38 and active β-catenin protein levels (Fig. 3O) were significantly higher in IECs of $Apc^{\Delta 580}$-PD mice than their WT-littermates. Also, GW501516 treatment of $Apc^{\Delta 580}$ mice increased BMP7, p-TAK1, and active β-catenin protein levels in IECs of $Apc^{\Delta 580}$ mice (Fig. 3P). In contrast, PPARD KO or GSK3787 treatment decreased BMP7, p-TAK1, and active β-catenin protein levels in IECs of $Apc^{\Delta 580}$ mice (Fig. 3Q; Fig. S3E)

## PPARD promotes CRC invasiveness

The transformation to invasive CRC occurs in large adenomas (3). PPARD overexpression or pharmacological activation in IECs significantly increased (Fig. 2B, D, G, and J) while PPARD KO or pharmacological inhibition decreased (Fig. 2L and N) the number of large tumors in APC mutant mice. When tested for invasive intestinal tumors, 86% of $Apc^{\Delta 580}$-PD mice but only 16% of their littermate $Apc^{\Delta 580}$ mice had invasive tumors ($P = 0.029$) (Fig.

4A and B). The mean number of invasive tumors per mouse increased from 0.14 (95% CI: 0.2-0.49) in $Apc^{\Delta 580}$ mice to 2.29 (95% CI: 1-3.56) in $Apc^{\Delta 580}$-PD mice ($P = 0.0056$) (Fig. 4B). When APC mutation was delayed until the mice reached adulthood, invasive tumors developed in $Apc^{\Delta 580\text{-}TMX}$-PD mice but not in their $Apc^{\Delta 580\text{-}TMX}$ littermates (Fig. 4C).

To assess the clinical relevance of these findings, we compared PPARD expression in paired samples of human colorectal adenomas, CRC tumor centers and CRC invasive fronts in 41 patients. Immunohistochemistry composite expression scores (CES) of PPARD expression were significantly higher in CRC invasive fronts than in their paired CRC tumor centers or adenomas (Fig. 4D and E; Table S1).

β-catenin nuclear localization in invasive front cells has been implicated as a mechanism for CRC invasiveness (22). We therefore measured β-catenin expression in the same paired human CRC sections used for PPARD IHC and found that while the total active β-catenin expression was higher in invasive fronts than paired adenomas in 76.9% of the cases, only approximately 22% of the cases had higher β-catenin nuclear expression levels in invasive fronts than in paired tumor centers (Fig. S4A and B; Table S1). 13 out of 32 CRCs without nuclear β-catenin upregulation in invasive fronts had PPARD upregulation in invasive fronts compared to paired tumor centers (Table S2), which suggested that PPARD might promote CRC invasiveness via additional mechanisms beyond modulating β-catenin nuclear localization. CT26 is a mouse CRC line that lacks APC and β-catenin mutations but exhibits aggressive and undifferentiated phenotype (23). We used CT26 to examine the effect of PPARD expression/activity modulation on CT26 cell invasion. PPARD overexpression in CT26 significantly increased CT26 cell invasion while GSK3787 blocked PPARD's promotion of cell invasion (Fig. 4F).

## Identification of PPARD downstream targets to promote CRC invasiveness

We screened for the downstream target genes of PPARD that promoted intestinal tumor invasiveness using comparative functional proteomics RPPA analyses of IECs from $Apc^{\Delta 580}$ and $Apc^{\Delta 580}$-PD mice that have the same APC mutation background. $Apc^{\Delta 580}$-PD and $Apc^{\Delta 580}$ mice had different proteomic patterns (Fig. 5A). Volcano plot analyses identified 7 differentially expressed proteins with at least a 2-fold expression change and 2-sided *t*-test *P* values of < 0.05. Six of these proteins were upregulated (connexin 43, AKT serine/threonine kinase 1 [AKT1], platelet-derived growth factor receptor β [PDGFRβ], cyclin-dependent kinase 1 [CDK1], eukaryotic translation initiation factor 4γ [EIF4G1], and phosphorylated ribosomal protein S6 [rpS6] at residues 235/236 and 240/244), while only 1 protein (caspase 7-cleaved) was downregulated (Fig. 5B).

## PPARD upregulates PDGFRβ expression in IECs

Independent experiments confirmed PPARD upregulation of PDGFRβ protein and mRNA expression in $Apc^{\Delta 580}$-PD mice (Fig. 5C and D) and PD mice (Fig. 5E and F). In clinical relevance assessments of these findings, PPARD and PDGFRβ mRNA levels were concomitantly higher in CRC tissues than in paired normal tissues in 20 of 22 colorectal cancer patients. (Fig. 5G and H). In The Cancer Genome Atlas (TCGA) provisional colorectal cancer database, PDGFRβ and PPARD mRNA levels were significantly

correlated, with a tendency towards co-occurrence (log odds ratio = 2.348; $P < 0.0001$) (Fig. 5I). PPARD overexpression in CT26 cells significantly increased cell migration and DMPQ (a specific PDGFRβ inhibitor) (24) reduced PPARD promotion of cell migration (Fig. 5J).

### PPARD activates AKT1/p-rpS6 signaling in IECs

PPARD upregulated AKT1 protein and mRNA expression in PD and $Apc^{\Delta 580}$-PD mice in independent confirmatory experiments (Fig. 6A-D). In contrast, AKT2 expression remained unchanged (Fig. 6A and B; Fig. S5A and B). PPARD also increased AKT1 phosphorylation and activation as measured by phosphorylation levels of AKT1, and downstream target proteins rpS6 and glycogen synthase kinase 3β (GSK3β) (Fig. 6A and B; Fig. S5C and D). Interrogation of TCGA colorectal cancer showed strong correlation between PPARD and AKT1 mRNA expression levels (Fig. 6E). PPARD overexpression in HCT116 cells increased AKT1 mRNA and protein expression and phosphorylation (Fig. 6F and G), while PPARD KO in KO1 cells decreased AKT1 and p-rpS6 expression levels (Fig. S5E). PPARD downregulation using 2 independent PPARD siRNAs in SW480 cells reduced AKT1 mRNA and protein levels and phosphorylation (Fig. 6H and I). PPARD overexpression increased PPARD binding to an in-silico predicted pPDBS in AKT1 promoter in SW480 cells (Fig. 6J and K). Finally, an AKT-selective inhibitor, MK2206 significantly inhibited cell migration promotion by PPARD overexpression in HCT116 cells (Fig. 6L).

### PPARD promotes intestinal tumorigenesis via upregulation of EIF4G1 and CDK1 in IECs

Independent follow-up experiments confirmed RPPA results that CDK1 and EIF4G1 protein expression was significantly higher not only in $Apc^{\Delta 580}$-PD mice but also in PD mice than in their control littermates (Fig. 7A and B). Because EIF4G1 is critical to the initiation of protein translation (25), we investigated whether intestinal PPARD overexpression increased protein translation by measuring ribosomal RNA. Intestinal PPARD overexpression markedly increased ribosomal RNA levels in both PD and $Apc^{\Delta 580}$-PD mice compared to their control littermates (Fig. S6A). The clinical relevance of PPARD upregulation of EIF4G1 and CDK1 in mouse IECs was assessed by measuring EIF4G1 and CDK1 expression in the same 41 paired colorectal adenomas, CRC tumor centers and CRC invasive fronts as used for PPARD and active β-catenin studies. EIF4G1 IHC scores were significantly higher in CRCs than in paired adenomas, and also in invasive fronts than paired tumor centers (Fig. 7C and D; Table S1). EIF4G1 upregulation was significantly correlated with PPARD upregulation in invasive fronts (Fig. 7E). Similarly, the percentage of positive CDK1 nuclear IHC staining was significantly higher in CRCs than in paired adenomas (Fig. S6B and C; Table S1). Mechanistically, PPARD downregulation by siRNA significantly decreased EIF4G1 (Fig. 7F) and CDK1 (Fig. 7G) mRNA expression in primary human CRC organoids. Furthermore, treatment with 4EGI-1, a specific inhibitor of EIF4G1 interaction with EIF4E, or CDK1 inhibitor RO-3306 suppressed PPARD overexpression promotion of cell invasion and migration in CT26 cells (Fig. 7H and7I).

## DISCUSSION

We found that PPARD potentiated β-catenin activation in IECs via upregulation of BMP7/TAK1 signaling and promoted CRC progression and invasion by also upregulating multiple

other important pro-tumorigenic proteins, including PDGFRβ, AKT1, EIF4G1, and CDK1 (Fig. 7J).

Our findings clearly address the controversy regarding PPARD's effects on β-catenin promotion of CRC. These new data from mutliple *in vivo* and *in vitro* models with genetic or pharmacological modulations of PPARD expression and activation clearly demonstrate that PPARD increases β-catenin activation to upregulate the expression of tumorigenic genes. The findings in PD mice without APC mutations and the data obtained from APC-WT HCT116 cells indicate that PPARD activation of β-catenin occurs at downstream of APC mutations. While APC mutations and subsequent aberrant β-catenin activation in intestinal stem cells is sufficient to initiate CRC (26), β-catenin activation occurs in varying degrees within an individual CRC with the same APC mutation background (22). This β-catenin activation variability has been interpreted to reflect additional modifiable factors that promote the transformation of CRC initiating stem cells via hyper-activation of β-catenin that regulates critical phenotypic features of CRC stem cells such as self-renewal (27). Our findings support the notion that PPARD is one of these modifiable factors that enhance β-catenin activation. Indeed, PPARD upregulation in mouse IECs increased β-catenin activation and subseqently increased intestinal progenitor cell self-renewal, especially in the form of immature spheroid organoids. The relvance of the mouse studies to human CRC is supported by our fidndings that PAPRD potentiated β-catenin activity, upregulated β-catenin downstream-target pro-tumorigenic genes (Axin-2, c-Myc, cyclin D1), and increased CRC stem cell self-renewal in primary human CRC organoids. While PPARD activation via high-fat diet or pharmaceutical ligands has been reported to enhance intestinal organoid formation in IECs of $Apc^{min}$ mice (12), our findings demonstrate for the first time that PPARD is sufficient not only to enhance intestinal progenitor cell self-renewal even without APC mutations in mouse IECs, but also regulates β-catenin signaling and progenitor cell self-renewal in human CRC organoids.

PPARD strongly promotes APC-mutation-driven CRC tumorigenesis. PPARD promotion of APC-mutation-driven CRC tumorigenesis is clearly supported by our findings from various APC mutation mouse models in which PPARD was either genetcially overexpressed or deleted in IECs or pharmacologically activated or inhibited. In contrast, prior studies were mainly limited to models of PPARD KO in $Apc^{min}$ mice. We tested PPARD's effects not only in $Apc^{min}$ mice, which develop small intestinal adenomas, but also in $Apc^{\Delta 580}$ mice, in which intestinally targeted APC mutations produces large intestinal CRC and thus better simulate human CRC. Furthermore, we tested the effects of genetically targeted PPARD overexpression into IECs to better simulate human CRC in which PPARD is predominately upregulated in CRC (6-8), not deleted or mutated (Fig. S7A). In contrast to the conflicting data from experiments with $Apc^{min}$ mice with germline PPARD KO (10,11), in all of our models, PPARD strongly potentiated APC-mutation-driven CRC. While genetic overexpression of PPARD in IECs might be criticized because the observed effects might be related to super-physiological overexpression levels, our findings also included ones from other complementary genetic and pharmacological mouse experimental models, in which, targeted PPARD KO in IECs inhibited, PPARD agonist GW501516 promoted, and PAPRD antagonist GSK3787 suppressed intestinal tumorigenesis in $Apc^{\Delta 580}$ mice. Others have reported that GW501516 significantly increased tumorigenesis in small intestines but not

large intestines of $Apc^{min}$ mice (28). We however used $Apc^{\Delta 580}$ mice, in which GW501516 significantly promoted large intestine tumorigenesis. Our data also showed for the first time that a PPARD inhibitor, GSK3787, suppressed colorectal tumorigenesis *in vivo*. Furthermore, our novel $Apc^{\Delta 580\text{-}TMX}$ mouse model, in which the onset of APC mutation is delayed to early adulthood to better simulate the delay in APC mutation occurrence in the common human CRC pattern, showed even more striking pro-tumorigenic effects of PPARD overexpression in IECs. Thus, our in-depth experimental modulations of intestinal PPARD in relation to APC mutations clearly establishes PPARD's role in promoting APC mutation-driven intestinal tumorigenesis.

PPARD transcriptionally upregulates BMP7 to activateTAK1/β-catenin signaling in IECs. The BMP7/TAK1 signaling pathway increases β-catenin activation and contributes to therapeutic resistance in APC- and KRAS-mutant CRC cells (e.g., SW620) (21). We have clearly demonstrated for the first time that PPARD activated BMP7/TAK1/β-catenin signaling not only in CRC cells with APC and KRAS mutations (i.e., SW620, SW480 cells) or with WT APC and mutant KRAS (i.e., HCT116 cells), but also *in vivo* in mice with and without APC mutations (PD and $Apc^{\Delta 580}$-PD mice), and more importantly in primary human CRC organoids. Prior reports have been inconsistent regarding PPARD's relation to TAK1. PPARD agonists have been reported to inhibit TAK1 phosphorylation in rodent renal tubular (29) and peritoneal mesothelial cells (30). However, PPARD downregulation or overexpression failed to alter the agonist's effects (29), thus indicating that non-PPARD-mediated mechanisms were involved. Others have questioned whether PPARD affects TAK1 activity because PPARD downregulation via siRNA in HeLa cells reduced TAK1 phosphorylation, whereas PPARD overexpression in HEK293T cells failed to increase TAK1 phosphorylation (31). While these different findings might be attributed to experimental differences, including using different experimental organs, our new data clearly showed that PPARD increased TAK1 phosphorylation in both *in vitro* and *in vivo* PPARD gain- and loss-of-function models. Moreover, our results elucidated the mechanism by which PPARD regulated TAK1 via transcriptional upregulation of BMP7. BMP7, upregulated/amplified in 16%-24% of human CRCs in the cBioPortal databases (Fig. S7B), negatively affects CRC patients' survival (Fig. S7C and D) and promotes CRC invasiveness (32). TAK1 phosphorylation is being investigated clinically as a molecular target in the treatment of human cancers (33). Our identification of PPARD, a druggable protein, as a regulator of the BMP7/TAK1 signaling pathway suggests a novel potential approach to targeting BMP7/TAK1 signaling.

PPARD promotes CRC invasiveness. In our various tested mouse models, PPARD promoted especially the formation of large intestinal tumors, in which invasive CRC typically occurs (3). Our subsequent findings strongly supported PPARD's role in promoting CRC invasiveness. While APC mutations are critical to CRC tumorigenesis initiation, APC mutations alone are insufficient to induce CRC invasiveness (3). We therefore used comparative protein expression analyses of $Apc^{\Delta 580}$-PD versus $Apc^{\Delta 580}$ mice that share the same APC mutation background to identify differentially regulated pro-tumorigenic targets by PPARD, which promoted CRC invasiveness in $Apc^{\Delta 580}$-PD. This screen identified several pro-invasive targets (e.g. PDGFRβ, AKT1, EIF4G1, and CDK1) as potential new PPARD's targets.

PPARD promoted CRC invasiveness via PDGFRβ and AKT1. We identified for the first time that PDGFRβ, a key gene in colorectal adenoma-to-carcinoma progression (34), is not only upregulated by PPARD in mice but also correlated with PPARD expression in human CRC. Additionally, PPARD promotion of CT26 cell migration was inhibited by selective PDGFRβ inhibitor DMPQ, confirming the mechanistic relevance of PDGFRβ to PPARD promotion of CRC invasiveness. The AKT/mTOR signaling pathway integrates various upstream oncogenic effector signals (e.g., PDGFRs) to modulate downstream targets (e.g., ribosomal protein S6 kinase 1 [S6K1], EIF4E binding proteins) and promote tumor progression and invasiveness (35). In particular, AKT increases β-catenin nuclear localization and tumor cell invasion (36). PPARD has been reported to activate AKT in mouse keratinocytes (37), A549 non-small cell lung cancer cells (38), and mammary epithelial cells (39). Our data demonstrate for the first time that: (1) PPARD specifically upregulates AKT1, but not AKT2, expression and phosphorylation in *in vitro* and *in vivo* CRC tumorigenesis models; (2) PPARD transcriptionally regulates AKT1; and (3) PPARD is strongly correlated with AKT1 expression in human CRC. In addition, PPARD also increased GSK3β phosphorylation, which enhances various tumorigenic mechanisms, especially aberrant β-catenin activation (40). PPARD agonists have been reported to increase AKT and GSK3β phosphorylation in rodent hearts challenged by ischemia or sepsis (41,42). Our data, however, show for the first time that PPARD increases GSK3β phosphorylation to drive CRC tumorigenesis. Our new data also demonstrated that PPARD upregulates connexin 43 in IECs *in vivo*, which is in agreement with our previously published *in vitro* data from differential transcriptome analyses of HCT116 and KO1 cells (8).

PPARD promoted CRC invasion via alternative mechanisms to increasing β-catenin nuclear localization. Enhancement of β-catenin nuclear localization beyond its activation by APC mutations is considered as an important mechanism to promote CRC invasiveness. This concept is based especially on observations that β-catenin nuclear localization is higher in human CRC invasive fronts than their paired tumor centers despite having the same APC mutation background (22). This increase in β-catenin nuclear localization has been reported to occur in 40%-89%of CRC invasive fronts in studies that were limited to well-differentiated CRCs (22,43). A more recent study reported that this differential β-catenin nuclear localization in invasive CRC fronts was observed in 26.92% of well-moderately-differentiated and 4.26% in poorly differentiated-mucinous CRC cases (44). Similar to this last report (44) , we found differential β-catenin nuclear localization in CRC invasive fronts in only 22% of our studied CRC cases. Our unselected CRC cases, unlike the other two prior studies (22,43), had 5% well-differentiated, 85% moderately-differentiated, and 10% poorly-differentiated CRCs. This distribution is relatively similar to the proportion expected in the general CRC patient population: 10% well-differentiated, 70% moderately differentiated, and 20% poorly differentiated (45). Differential β-catenin nuclear localization in CRC invasive fronts varied in our cases with CRC differentiation: 2/2 of well-differentiated, 7/35 of moderately differentiated, and 0/4 of poorly differentiated CRCs. Therefore, the majority of CRCs with moderately to poorly differentiated histology lacked this differential β-catenin nuclear localization in invasive fronts, which suggested that these CRCs employed the mechanisms other than β-catenin nuclear localization to promote invasiveness. We found that in 40.6% of these CRC cases without β-catenin nuclear localization in invasive fronts,

PPARD was differentially upregulated compared to paired tumor centers (Table S2), which suggests that PPARD promotes CRC invasiveness via additional mechanisms to β-catenin nuclear localization. In agreement with notion, PPARD overexpression in CT26 cells that lacks APC and β-catenin mutations significantly increased, while PPARD inhibitor GSK3787 significantly suppressed cancer cell invasion.

PPARD upregulated EIF4G1 and CDK1 to promote CRC invasiveness. Our data identified EIF4G1 and CDK1 as novel downstream targets of PPARD in mouse IECs and human CRC organoids to promote CRC invasiveness. EIF4G1, an essential scaffold protein for assembling EIF4F protein complex to initiate mRNA translation (46), plays an important role in cancer progression (47). CDK1 regulates cell cycle-dependent (e.g., chromosome segregation, DNA repair) (48) and -independent (e.g., protein translation independent of AKT) (49) functions to promote tumorigenesis progression (50). Dysregulation of mRNA translation promotes tumorigenesis progression via multiple mechanisms that are unrestricted to β-catenin (46). In our study, EIF4G1 and nuclear CDK1 nuclear localization were differentially upregulated in CRC invasive fronts in 53.1%, and 31.3% of CRC cases that lacked nuclear β-catenin localization (Table S2). These finding support the potential roles of EIF4G1 and CDK1 as alternative mechanisms to nuclear β-catenin localization in promoting CRC invasiveness. Specific inhibition of EIF4G1 interaction with EIF4E by EIF4G1 inhibitor 4EGI-1 or CDK1 pharmacological inhibition suppressed PPARD promotion of CT26 cell invasion and migration, which further support the roles of EIF4G1 and CDK1 in promoting CRC invasiveness.

In conclusion, our findings demonstrate that PPARD strongly accelerates APC mutation-driven CRC progression and invasion via multiple important pro-tumorigenic pathways, including BMP7/TAK1/β-catenin, PDGFRβ, AKT1, EIF4G1, and CDK1 (Fig. 7J). These findings establish PPARD's pivotal role in promoting CRC progression and its potential as a preventive and therapeutic target.

## Supplementary Material

Refer to Web version on PubMed Central for supplementary material.

## ACKNOWLEDGMENTS

We thank Drs. Pierre McCrea and Jail Park for their feedback on this work. We thank MS. Amy Ninetto and Mr. Bryan Tutt at the Department of Scientific Publications at MD Anderson Cancer Center for editing the manuscript.

**Financial Support:** This work was supported by the Cancer Prevention and Research Institute of Texas (RP140224 to I.S) and the National Cancer Institute (R01-CA142969, R01-CA195686, and R01-CA206539 to I.S.). This study made use of the MD Anderson Cancer Center Genetically Engineered Mouse Facility, Functional Proteomics Reverse-Phase Protein Array Core, Sequencing and Microarray Facility, and Research Animal Support Facility at Houston, supported by Cancer Center Support Grant CA016672.

## REFERENCES

1. Morin PJ, Sparks AB, Korinek V, Barker N, Clevers H, Vogelstein B, et al. Activation of β-Catenin-Tcf Signaling in Colon Cancer by Mutations in β-Catenin or APC. Science 1997;275:1787–90 [PubMed: 9065402]

2. Fearon ER, Vogelstein B. A genetic model for colorectal tumorigenesis. Cell 1990;61:759–67 [PubMed: 2188735]
3. Oshima H, Nakayama M, Han TS, Naoi K, Ju X, Maeda Y, et al. Suppressing TGFbeta signaling in regenerating epithelia in an inflammatory microenvironment is sufficient to cause invasive intestinal cancer. Cancer Res 2015;75:766–76 [PubMed: 25687406]
4. Haggitt RC, Glotzbach RE, Soffer EE, Wruble LD. Prognostic factors in colorectal carcinomas arising in adenomas: Implications for lesions removed by endoscopic polypectomy. Gastroenterology 1985;89:328–36 [PubMed: 4007423]
5. Michalik L, Desvergne B, Wahli W. Peroxisome-proliferator-activated receptors and cancers: complex stories. Nat Rev Cancer 2004;4:61–70 [PubMed: 14708026]
6. He TC, Chan TA, Vogelstein B, Kinzler KW. PPARdelta is an APC-regulated target of nonsteroidal anti-inflammatory drugs. Cell 1999;99:335–45 [PubMed: 10555149]
7. Takayama O, Yamamoto H, Damdinsuren B, Sugita Y, Ngan CY, Xu X, et al. Expression of PPAR[delta] in multistage carcinogenesis of the colorectum: implications of malignant cancer morphology. Br J Cancer 2006;95:889–95 [PubMed: 16969348]
8. Zuo X, Xu W, Xu M, Tian R, Moussalli MJ, Mao F, et al. Metastasis regulation by PPARD expression in cancer cells. JCI Insight 2017;2:e91419 [PubMed: 28097239]
9. Foreman JE, Sorg JM, McGinnis KS, Rigas B, Williams JL, Clapper ML, et al. Regulation of peroxisome proliferator-activated receptor-β/δ by the APC/β-CATENIN pathway and nonsteroidal antiinflammatory drugs. Mol Carcinog 2009;48:942–52 [PubMed: 19415698]
10. Harman FS, Nicol CJ, Marin HE, Ward JM, Gonzalez FJ, Peters JM. Peroxisome proliferator-activated receptor-delta attenuates colon carcinogenesis. Nat Med 2004;10:481–3 [PubMed: 15048110]
11. Wang D, Wang H, Guo Y, Ning W, Katkuri S, Wahli W, et al. Crosstalk between peroxisome proliferator-activated receptor delta and VEGF stimulates cancer progression. Proc Natl Acad Sci U S A 2006;103:19069–74 [PubMed: 17148604]
12. Beyaz S, Mana MD, Roper J, Kedrin D, Saadatpour A, Hong SJ, et al. High-fat diet enhances stemness and tumorigenicity of intestinal progenitors. Nature 2016;531:53–8 [PubMed: 26935695]
13. Peters JM, Gonzalez FJ, Müller R. Establishing the Role of PPARβ/δ in Carcinogenesis. Trends Endocrinol Metab 2015;26:595–607 [PubMed: 26490384]
14. Hinoi T, Akyol A, Theisen BK, Ferguson DO, Greenson JK, Williams BO, et al. Mouse Model of Colonic Adenoma-Carcinoma Progression Based on Somatic Apc Inactivation. Cancer Res 2007;67:9721–30 [PubMed: 17942902]
15. Zuo X, Xu M, Yu J, Wu Y, Moussalli MJ, Manyam GC, et al. Potentiation of colon cancer susceptibility in mice by colonic epithelial PPAR-delta/beta overexpression. J Natl Cancer Inst 2014;106:dju052 [PubMed: 24681603]
16. Hung KE, Maricevich MA, Richard LG, Chen WY, Richardson MP, Kunin A, et al. Development of a mouse model for sporadic and metastatic colon tumors and its use in assessing drug treatment. Proc Natl Acad Sci U S A 2010;107:1565–70 [PubMed: 20080688]
17. Barak Y, Liao D, He W, Ong ES, Nelson MC, Olefsky JM, et al. Effects of peroxisome proliferator-activated receptor delta on placentation, adiposity, and colorectal cancer. Proc Natl Acad Sci U S A 2002;99:303–8 [PubMed: 11756685]
18. Sato T, Stange DE, Ferrante M, Vries RG, Van Es JH, Van den Brink S, et al. Long-term expansion of epithelial organoids from human colon, adenoma, adenocarcinoma, and Barrett's epithelium. Gastroenterology 2011;141:1762–72 [PubMed: 21889923]
19. Li J, Akbani R, Zhao W, Lu Y, Weinstein JN, Mills GB, et al. Explore, Visualize, and Analyze Functional Cancer Proteomic Data Using the Cancer Proteome Atlas. Cancer Res 2017;77:e51–e4 [PubMed: 29092939]
20. Schwitalla S, Fingerle Alexander A, Cammareri P, Nebelsiek T, Göktuna Serkan I, Ziegler Paul K, et al. Intestinal Tumorigenesis Initiated by Dedifferentiation and Acquisition of Stem-Cell-like Properties. Cell 2013;152:25–38 [PubMed: 23273993]
21. Singh A, Sweeney Michael F, Yu M, Burger A, Greninger P, Benes C, et al. TAK1 Inhibition Promotes Apoptosis in KRAS-Dependent Colon Cancers. Cell 2012;148:639–50 [PubMed: 22341439]

22. Brabletz T, Jung A, Reu S, Porzner M, Hlubek F, Kunz-Schughart LA, et al. Variable beta-catenin expression in colorectal cancers indicates tumor progression driven by the tumor environment. Proc Natl Acad Sci U S A 2001;98:10356–61 [PubMed: 11526241]
23. Castle JC, Loewer M, Boegel S, de Graaf J, Bender C, Tadmor AD, et al. Immunomic, genomic and transcriptomic characterization of CT26 colorectal carcinoma. BMC Genomics 2014;15:190 [PubMed: 24621249]
24. Dolle RE, Dunn JA, Bobko M, Singh B, Kuster JE, Baizman E, et al. 5,7-Dimethoxy-3-(4-Pyridinyl)Quinoline Is a Potent and Selective Inhibitor of Human Vascular .beta.-Type Platelet-Derived Growth Factor Receptor Tyrosine Kinase. J Med Chem 1994;37:2627–9 [PubMed: 8064792]
25. Jackson RJ, Hellen CUT, Pestova TV. The mechanism of eukaryotic translation initiation and principles of its regulation. Nature Reviews Molecular Cell Biology 2010;11:113 [PubMed: 20094052]
26. Barker N, Ridgway RA, van Es JH, van de Wetering M, Begthel H, van den Born M, et al. Crypt stem cells as the cells-of-origin of intestinal cancer. Nature 2008;457:608 [PubMed: 19092804]
27. Vermeulen L, De Sousa EMF, van der Heijden M, Cameron K, de Jong JH, Borovski T, et al. Wnt activity defines colon cancer stem cells and is regulated by the microenvironment. Nat Cell Biol 2010;12:468–76 [PubMed: 20418870]
28. Gupta RA, Wang D, Katkuri S, Wang H, Dey SK, DuBois RN. Activation of nuclear hormone receptor peroxisome proliferator-activated receptor-delta accelerates intestinal adenoma growth. Nat Med 2004;10:245–7 [PubMed: 14758356]
29. Yang X, Kume S, Tanaka Y, Isshiki K, Araki S-i, Chin-Kanasaki M, et al. GW501516, a PPARδ Agonist, Ameliorates Tubulointerstitial Inflammation in Proteinuric Kidney Disease via Inhibition of TAK1-NFκB Pathway in Mice. PLoS One 2011;6:e25271 [PubMed: 21966476]
30. Su X, Zhou G, Wang Y, Yang X, Li L, Yu R, et al. The PPARβ/δ Agonist GW501516 Attenuates Peritonitis in Peritoneal Fibrosis via Inhibition of TAK1–NFκB Pathway in Rats. Inflammation 2014;37:729–37 [PubMed: 24337677]
31. Stockert J, Wolf A, Kaddatz K, Schnitzer E, Finkernagel F, Meissner W, et al. Regulation of TAK1/TAB1-Mediated IL-1β Signaling by Cytoplasmic PPARβ/δ. PLoS One 2013;8:e63011 [PubMed: 23646170]
32. Grijelmo C, Rodrigue C, Svrcek M, Bruyneel E, Hendrix A, de Wever O, et al. Proinvasive activity of BMP-7 through SMAD4 /src -independent and ERK/ Rac /JNK -dependent signaling pathways in colon cancer cells. Cell Signal 2007;19:1722–32 [PubMed: 17478078]
33. Tan L, Gurbani D, Weisberg EL, Hunter JC, Li L, Jones DS, et al. Structure-guided development of covalent TAK1 inhibitors. Bioorg Med Chem 2017;25:838–46 [PubMed: 28011204]
34. Sillars-Hardebol A, Carvalho B, de Wit M, Postma C, Delis-van Diemen P, Mongera S, et al. Identification of key genes for carcinogenic pathways associated with colorectal adenoma-to-carcinoma progression. Tumor Biol 2010;31:89–96
35. Hay N, Sonenberg N. Upstream and downstream of mTOR. Genes Dev 2004;18:1926–45 [PubMed: 15314020]
36. Fang D, Hawke D, Zheng Y, Xia Y, Meisenhelder J, Nika H, et al. Phosphorylation of β-Catenin by AKT Promotes β-Catenin Transcriptional Activity. J Biol Chem 2007;282:11221–9 [PubMed: 17287208]
37. Di-Poi N, Ng CY, Tan NS, Yang Z, Hemmings BA, Desvergne B, et al. Epithelium-Mesenchyme Interactions Control the Activity of Peroxisome Proliferator-Activated Receptor {beta}/{delta} during Hair Follicle Development. Mol Cell Biol 2005;25:1696–712 [PubMed: 15713628]
38. Pedchenko TV, Gonzalez AL, Wang D, DuBois RN, Massion PP. Peroxisome proliferator-activated receptor beta/delta expression and activation in lung cancer. Am J Respir Cell Mol Biol 2008;39:689–96 [PubMed: 18566335]
39. Yuan H, Lu J, Xiao J, Upadhyay G, Umans R, Kallakury B, et al. PPARdelta induces estrogen receptor-positive mammary neoplasia through an inflammatory and metabolic phenotype linked to mTOR activation. Cancer Res 2013;73:4349–61 [PubMed: 23811944]

40. McCubrey JA, Steelman LS, Bertrand FE, Davis NM, Sokolosky M, Abrams SL, et al. GSK-3 as potential target for therapeutic intervention in cancer. Oncotarget 2014;5:2881–911 [PubMed: 24931005]

41. Kapoor A, Collino M, Castiglia S, Fantozzi R, Thiemermann C. ACTIVATION OF PEROXISOME PROLIFERATOR-ACTIVATED RECEPTOR-β/δ ATTENUATES MYOCARDIAL ISCHEMIA/REPERFUSION INJURY IN THE RAT. Shock 2010;34:117–24 [PubMed: 19997057]

42. Kapoor A, Shintani Y, Collino M, Osuchowski MF, Busch D, Patel NSA, et al. Protective Role of Peroxisome Proliferator-activated Receptor-β/δ in Septic Shock. Am J Respir Crit Care Med 2010;182:1506–15 [PubMed: 20693380]

43. Jung A, Schrauder M, Oswald U, Knoll C, Sellberg P, Palmqvist R, et al. The invasion front of human colorectal adenocarcinomas shows co-localization of nuclear beta-catenin, cyclin D1, and p16INK4A and is a region of low proliferation. The American journal of pathology 2001;159:1613–7 [PubMed: 11696421]

44. Gao Z-H, Lu C, Wang M-X, Han Y, Guo L-J. Differential β-catenin expression levels are associated with morphological features and prognosis of colorectal cancer. Oncol Lett 2014;8:2069–76 [PubMed: 25295092]

45. Fleming M, Ravula S, Tatishchev SF, Wang HL. Colorectal carcinoma: Pathologic aspects. J Gastrointest Oncol 2012;3:153–73 [PubMed: 22943008]

46. Ruggero D Translational control in cancer etiology. Cold Spring Harb Perspect Biol 2013;5

47. Sharma DK, Bressler K, Patel H, Balasingam N, Thakor N. Role of Eukaryotic Initiation Factors during Cellular Stress and Cancer Progression. Journal of Nucleic Acids 2016;2016:8235121 [PubMed: 28083147]

48. Enserink JM, Kolodner RD. An overview of Cdk1-controlled targets and processes. Cell Div 2010;5:11 [PubMed: 20465793]

49. Shuda M, Velásquez C, Cheng E, Cordek DG, Kwun HJ, Chang Y, et al. CDK1 substitutes for mTOR kinase to activate mitotic cap-dependent protein translation. Proceedings of the National Academy of Sciences 2015;112:5875–82

50. Brown NR, Korolchuk S, Martin MP, Stanley WA, Moukhametzianov R, Noble MEM, et al. CDK1 structures reveal conserved and unique features of the essential cell cycle CDK. Nature Communications 2015;6:6769

**Significance:**

Findings address long-standing, important, and unresolved questions related to the potential role of PPAR-delta in APC-mutation-dependent colorectal tumorigenesis by showing PPAR-delta activation enhances APC-mutation-dependent tumorigenesis.

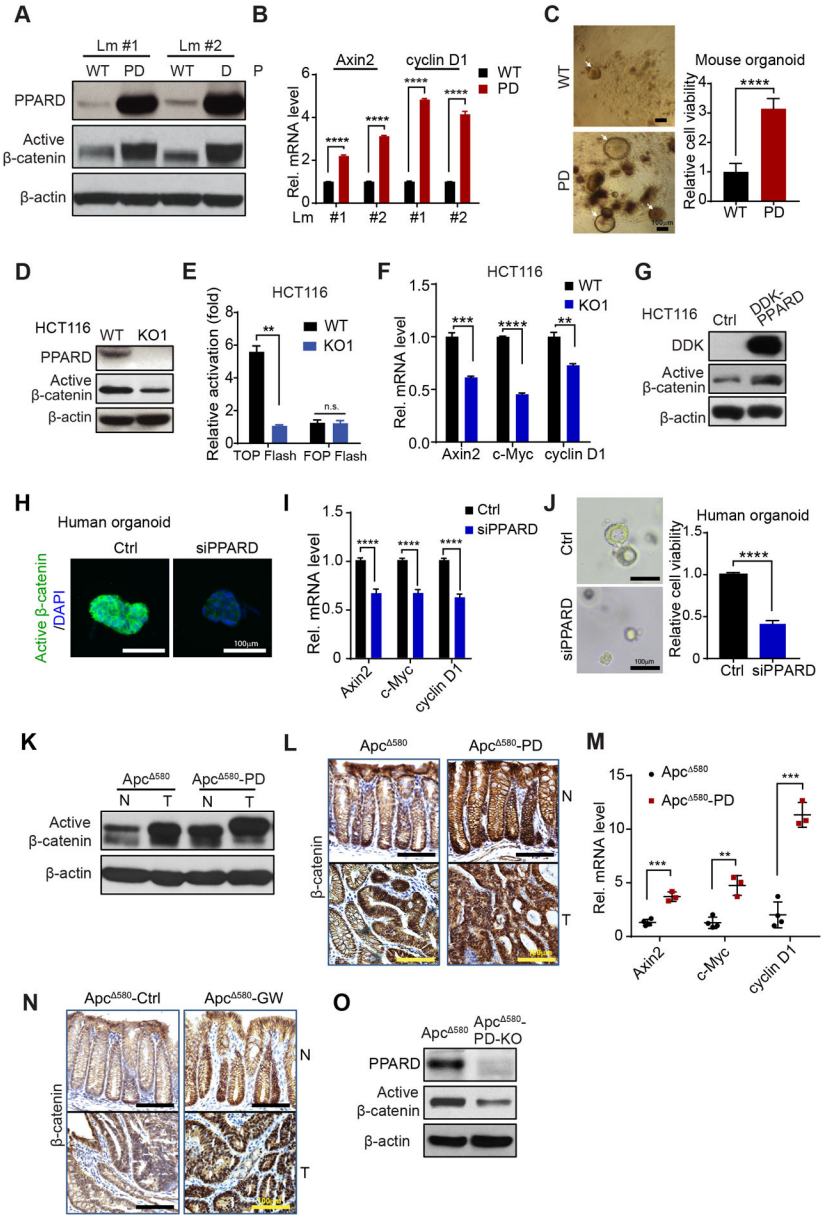


**Figure 1.**

PPARD activates β-catenin signaling in IECs. **A and B,** Active β-catenin protein levels (**A**) and mRNA levels of β-catenin target genes (Axin2 and cyclin D1) (**B**) in IECs of PD mice and WT littermates at age 10 weeks. Lm indicates littermate. **C,** The organoid-initiating capacity of IECs derived from PD mice and WT littermates at 6 weeks (n = 6 per group). Photomicrographs of primary organoids (**left**); and organoid cell viability measured by CellTiter-Glo Luminescent Cell Viability Assay (**right**). White arrows indicate individual organoids. **D-F,** Active β-catenin protein level (**D**), activity (**E**) and mRNA levels of Axin2, c-Myc, and cyclin D1 (**F**) in HCT116 cells without (WT) or with PPARD knockout (KO1). **G,** Active β-catenin protein levels of HCT116 cells stably transduced with control (Ctrl) or DDK-tagged PPARD (DDK-PPARD) lentiviral particles. **H-J,** Active β-catenin protein

expression (**H**), mRNA levels of Axin2, c-Myc, and cyclin D1 (**I**), and representative organoid images and organoid cell viability (**J**) in human organoid cells transfected with control siRNA (Ctrl) or PPARD siRNA (siPPARD) for 48 hours (**H and I**) or 96 hours (**J**) (n = 3). **K-M,** Active β-catenin protein expression in normal and tumor IECs by Western blot (**K**); expression and localization of β-catenin in colonic normal and tumor tissues IHC (**L**); and Axin2, c-Myc, and cyclin D1 mRNA expression levels in normal IECs (**M**) of $Apc^{\Delta 580}$ and $Apc^{\Delta 580}$-PD mice at age 14 weeks. **N,** $Apc^{\Delta 580}$ mice were fed a diet containing the PPARD agonist GW501516 (50 mg/kg) (GW) or a control diet (Ctrl) for 10 weeks, then evaluated for β-catenin expression by IHC. **O,** Active β-catenin protein expression in IECs of $Apc^{\Delta 580}$ and $Apc^{\Delta 580}$-PD-KO mice at age 14 weeks. Data are shown as mean ± SEM. ** *P < 0.01*, *** *P < 0.001*, and **** *P < 0.0001*.

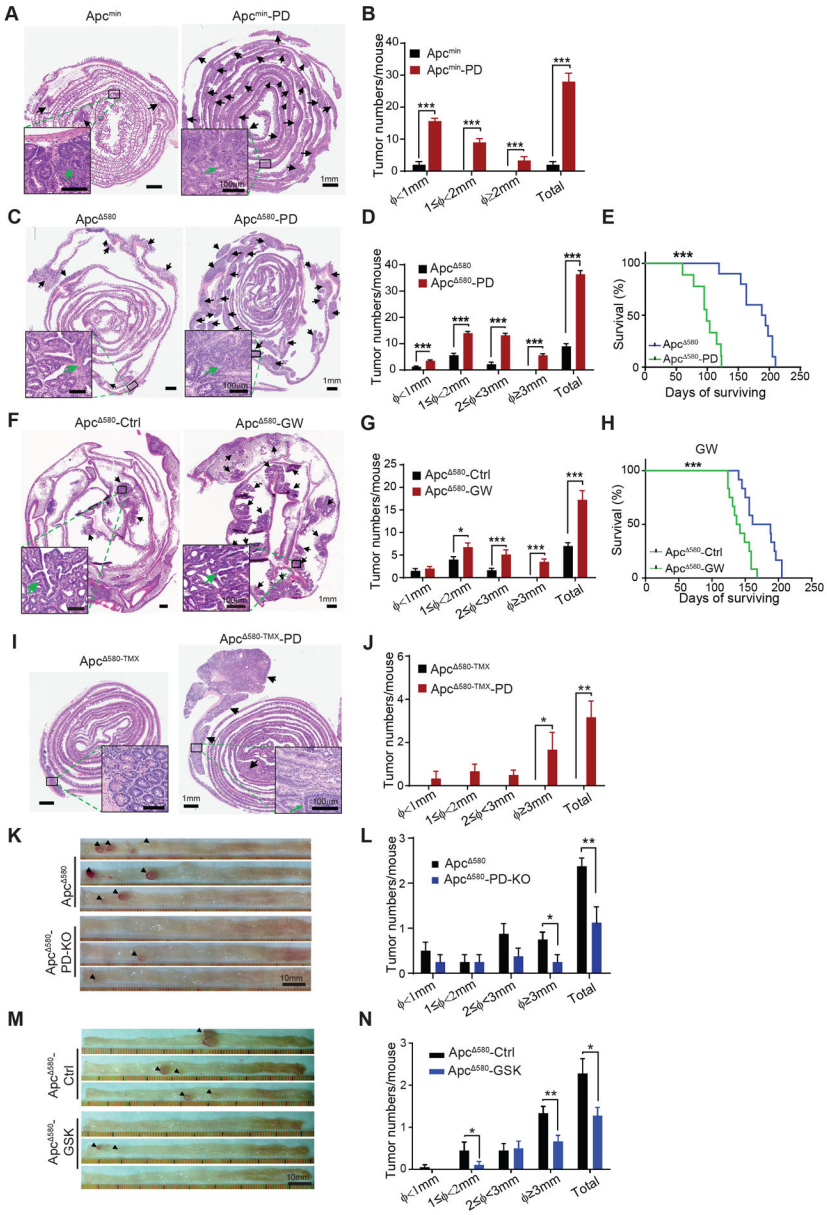


**Figure 2.**

PPARD accelerates APC mutation-driven intestinal tumorigenesis in mice. **A and B,** Effects of PPARD overexpression on intestinal tumorigenesis in $Apc^{min}$ mice. **A,** Representative images of H&E-stained intestines of $Apc^{min}$ mice and $Apc^{min}$-PD littermates at 8 weeks of age. Upper panel: Photomicrographs of whole-length intestinal sections (Swiss roll). Arrows indicate tumors. Lower panel: higher-magnification photomicrographs of tumor lesions. **B,** Intestinal tumor numbers and sizes for the indicated groups (n = 6 mice per group). Φ indicates tumor maximum diameter. **C-E,** Effects of PPARD overexpression on intestinal tumorigenesis in $APC^{\Delta 580}$ mice. **C,** Representative images of H&E-stained whole-length intestinal sections of $Apc^{\Delta 580}$ and $Apc^{\Delta 580}$-PD mice at 14 weeks of age. Upper and lower panel picture descriptions are similar to panel A. **D,** Intestinal tumor numbers and sizes for the indicated groups (n = 15 mice per group). **E,** Survival curves of $Apc^{\Delta 580}$ and $Apc^{\Delta 580}$-

PD mice (n = 20 mice per group). **F-H,** Effects of PPARD agonist GW501516 on intestinal tumorigenesis in $Apc^{\Delta 580}$ mice. **F,** $Apc^{\Delta 580}$ mice at age 4 weeks were fed a diet containing 50 mg/kg GW501516 ($Apc^{\Delta 580}$-GW) or a control diet ($Apc^{\Delta 580}$-Ctrl) for 10 weeks and then killed for intestinal tumorigenesis analyses. Upper and lower panel picture descriptions are similar to panel A. **G,** Intestinal tumor numbers and sizes for the indicated groups (n = 10 mice per group). **H,** Survival curves of the indicated groups (n = 12 mice per group). **I and J,** Effects of PPARD overexpression on intestinal tumorigenesis driven by adult-onset intestinally targeted APC mutation. $Apc^{\Delta 580}$ mutation was induced in the mice at age 6 weeks via tamoxifen-controlled Cre-recombinase expression driven by CDX-2 promoter ($Apc^{\Delta 580\text{-}TMX}$). $Apc^{\Delta 580\text{-}TMX}$ mice without or with intestinal PPARD overexpression ($Apc^{\Delta 580\text{-}TMX}$-PD) were followed for 55 weeks before they were killed for intestinal tumorigenesis analyses. **I,** Upper and lower panel picture descriptions are similar to panel A. **J,** Intestinal tumor numbers and sizes for the indicated groups (n = 8 mice per group). **K and L,** Effects of PPARD knockout/deletion on intestinal tumorigenesis in $APC^{\Delta 580}$ mice. Representative colon photographs (**K**) and colonic tumor numbers and sizes (**L**) of $Apc^{\Delta 580}$ and $Apc^{\Delta 580}$-PD-KO mice at 14 weeks of age (n = 8 mice per group). **M and N,** Effects of PPARD antagonist GSK3787 on intestinal tumorigenesis in $Apc^{\Delta 580}$ mice. $Apc^{\Delta 580}$ mice at age 4 weeks were fed a diet containing 200 mg/kg GSK3787 ($Apc^{\Delta 580}$-GSK) or a control diet ($Apc^{\Delta 580}$-Ctrl) for 12 weeks and then killed for intestinal tumorigenesis analyses. Representative colon photographs (**M**) and colonic tumor numbers and sizes (**N**) for the indicated groups (n = 18-20 mice per group). Data are shown as mean ± SEM. $*P < 0.05$, $**P < 0.01$, and $***P < 0.001$.

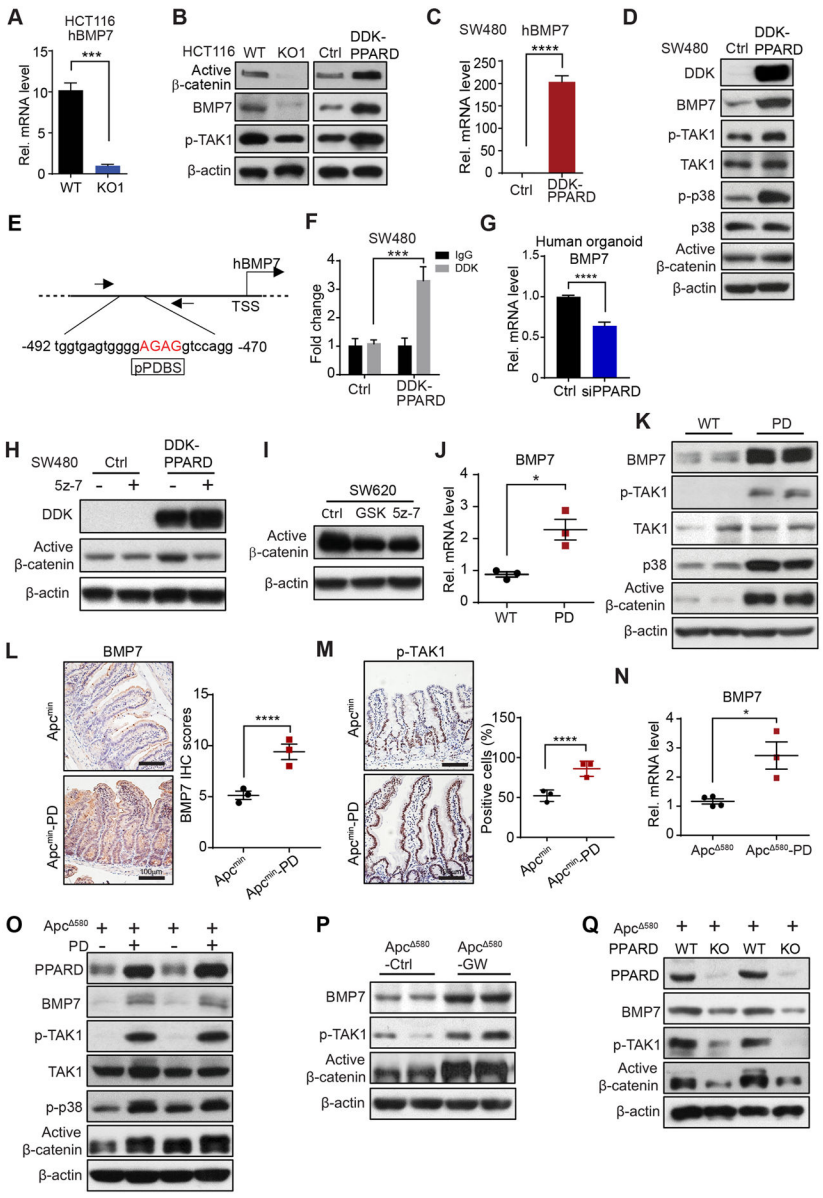


**Figure 3.**

PPARD activates BMP7/TAK1/β-catenin signaling in IECs. **A,** BMP7 mRNA expression levels in HCT116 WT or KO1 cells. **B,** Protein expression of BMP7, phosphorylated TAK1 (p-TAK1) in HCT116 WT or KO1 cells or HCT116 cells stably transduced with Ctrl or DDK-PPARD as described in Figure 1G. **C,** BMP7 mRNA expression levels in SW480 cells stably transduced with Ctrl or DDK-PPARD. **D,** Expression levels of BMP7, p-TAK1, TAK1, phosphorylated-p38 (p-p38), p38, and active β-catenin in SW480 cells described in panel C. **E,** Schematic map of potential PPARD binding site (pPDBS) in the promoter of the human BMP7 gene according to Genomatix MatInspector online software. Nucleotides marked in red indicate core sequences. TSS: transcription start site. **F,** PPARD's binding to pPDBS in the promoter of the human BMP7 gene, measured by chromatin immunoprecipitation-quantitative PCR (−492 to −470 bp of the BMP7 promoter) in SW480

cells described in panel C. **G,** BMP7 mRNA expression level in human CRC organoid cells transfected with Ctrl-siRNA or PPARD siRNA for 48 hours. **H,** Active β-catenin expression in SW480 cells described in panel C, treated with the specific TAK1 inhibitor 5z-7 (2.5 μM) or an equal amount of control solvent (DMSO) for 24 hours. **I,** Active β-catenin expression levels in SW620 cells treated with 5z-7 (2.5 μM), PPARD antagonist GSK3787 (GSK, 1 μM), or an equal amount of DMSO for 24 hours. **J,** BMP7 mRNA expression levels in IECs of PD mice and their WT littermates. **K,** Protein expression levels of the indicated genes in IECs of the mice described in panel J. **L and M,** Representative IHC images and IHC scores of BMP-7 (**L**) and p-TAK1 (**M**) expression in IECs of the $Apc^{min}$ and $Apc^{min}$-PD mice at 8 weeks (n = 3 mice/group). IHC CES of BMP-7 and average percentage of positive IHC stained cells of p-TAK1 obtained from 20 glands were presented. **N,** BMP7 mRNA expression levels in IECs of $Apc^{\Delta 580}$ and $Apc^{\Delta 580}$-PD littermates. **O,** Protein expression levels of the indicated genes in IECs of the mice described in panel N. **P,** Protein expression levels of the indicated genes in IECs of $Apc^{\Delta 580}$ mice treated with GW501516 or control diet as described in Figure 2F-H. **Q,** Protein expression levels of the indicated genes in IECs of $Apc^{\Delta 580}$ and $Apc^{\Delta 580}$-PD-KO mice. Data are shown as mean ± SEM. $*P < 0.05$, $***P < 0.001$, and $****P < 0.0001$.

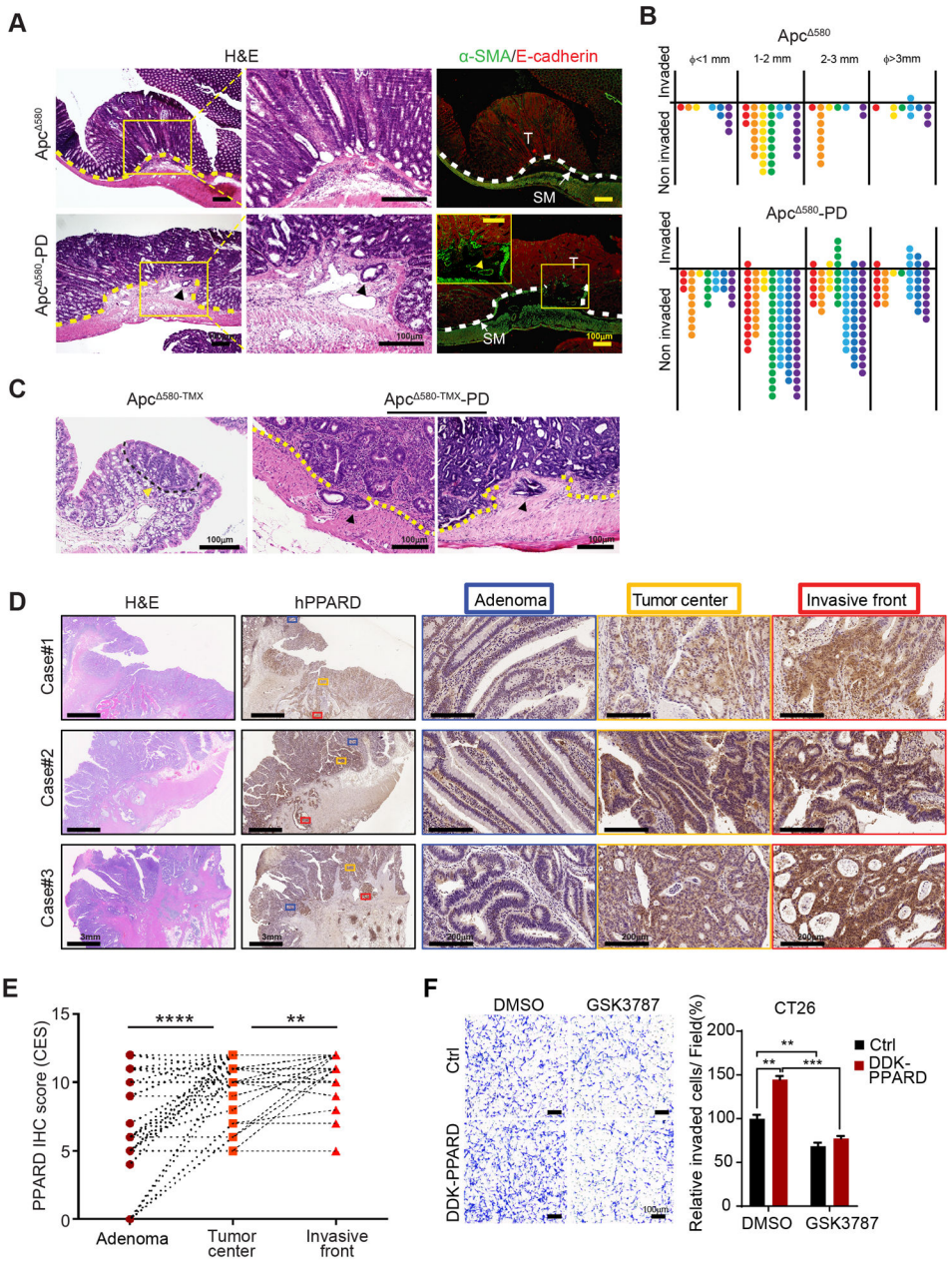


**Figure 4.**

PPARD promotes intestinal tumor invasion. **A and B,** Intestinal PPARD overexpression promotes invasion of intestinal tumors in $Apc^{\Delta 580}$ mice. Intestines of $Apc^{\Delta 580}$ and $Apc^{\Delta 580}$-PD littermate mice (20 weeks old) were evaluated for tumor invasiveness. **A,** Representative intestinal section photographs of noninvasive adenoma (upper) and invasive adenocarcinoma (lower) in the indicated mouse groups. Photomicrographs of low (left) and high (middle) magnifications of H&E staining and immunofluorescence staining (right) for E-cadherin (red) and α-SMA (green). T, tumor; SM, submucosa. **B,** Numbers of invasive and noninvasive tumors per mouse for the indicated groups, scored in whole-mount intestinal (Swiss roll) sections (n = 7 mice/group). **C,** $Apc^{\Delta 580}$ mutation was induced by tamoxifen

treatment of littermate mice without ($Apc^{\Delta 580\text{-}TMX}$) or with intestinal PPARD overexpression ($Apc^{\Delta 580\text{-}TMX}$-PD) at 6 weeks of age. Mice were followed for 55 weeks prior to being killed to assess intestinal tumor invasiveness. H&E staining photomicrographs showing the only microscopically identified adenoma in the $Apc^{\Delta 580\text{-}TMX}$ group and 2 representative invasive adenocarcinomas in the $Apc^{\Delta 580\text{-}TMX}$-PD group. **D and E**, PPARD expression in human colorectal cancer invasive fronts. **D,** Representative PPARD IHC staining images of human paired colorectal adenomas (Adenoma), CRC tumor centers (Tumor center), and CRC invasive fronts (Invasive front) of 3 patients. **E,** Total combined CES of nucleus and cytoplasm IHC staining of PPARD for the paired adenomas, CRC tumor centers, and CRC invasive fronts as described in panel D (n = 41 patients). **F,** Effects of PPARD inhibitor GSK3787 on PPARD promotion of CT26 mouse CRC cell invasion. CT26 cells stably transduced with a control (Ctrl) or mouse DDK-PPARD lentiviral particles were treated with GSK3787 (1.0 μM) or vehicle solvent (DMSO) for 48 hours. **Left:** representative photomicrographs of invaded cells. **Right:** invaded cells in at least 4 random individual fields per insert membrane were counted. Data are shown as mean ± SEM. $^{**}P < 0.01$, $^{***}P < 0.001$, and $^{****}P < 0.0001$.

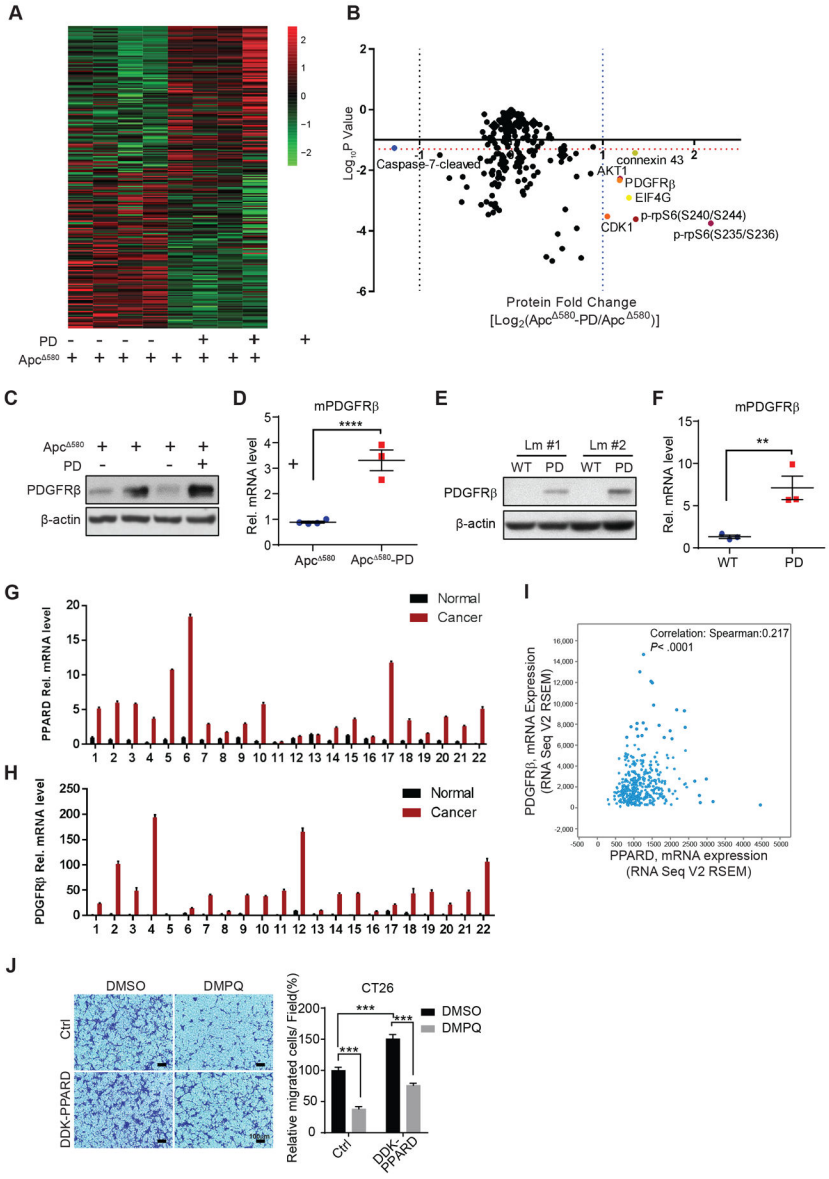


**Figure 5.**

PPARD transcriptionally upregulates PDGFRβ expression in IECs. **A and B,** RPPA analyses were performed on normal intestinal epithelial cells (IECs) of $Apc^{\Delta 580}$ and $Apc^{\Delta 580}$-PD littermate mice at 10 weeks of age (n = 4 mice per group). Results are presented as a heat map (**A**) and a volcano plot of the differentially expressed genes (**B**). The horizontal orange dotted line indicates the threshold, $P = 0.05$. The vertical blue dotted line on the right indicates where the $\log_2$ ratio was > 1, and the vertical dotted line on the left indicates where the $\log_2$ ratio was < −1. **C-F,** Effects of PPARD overexpression on PDGFRβ protein and mRNA expression levels in IECs of $APC^{\Delta 580}$ and $APC^{\Delta 580}$-PD (**C and D**) and PD and WT littermate (Lm) mice (**E and F**). **G and H,** PPARD (**G**) and PDGFRβ (**H**) mRNA levels in paired patient colorectal cancer and normal mucosa samples (n = 22). **I,** Spearman correlation analysis of PPARD and PDGFRβ mRNA expression in the TCGA provisional colorectal adenocarcinoma database (n = 633). **J,** Effects of PDGFRβ inhibitor DMPQ on

PPARD promotion of colon cancer cell migration. CT26 mouse colon cancer cells stably transduced with a mouse DDK-PPARD or control (Ctrl) lentiviral particles were treated with DMPQ (1.0 μM) or vehicle solvent (DMSO) for 36 hours. **Left:** representative photomicrographs of migrated cells. **Right:** migrated cells in at least 4 random individual fields per insert membrane were counted. Data are shown as mean ± SEM. $^{**}P < 0.01$, $^{***}P < 0.01$, and $^{****}P < 0.0001$.

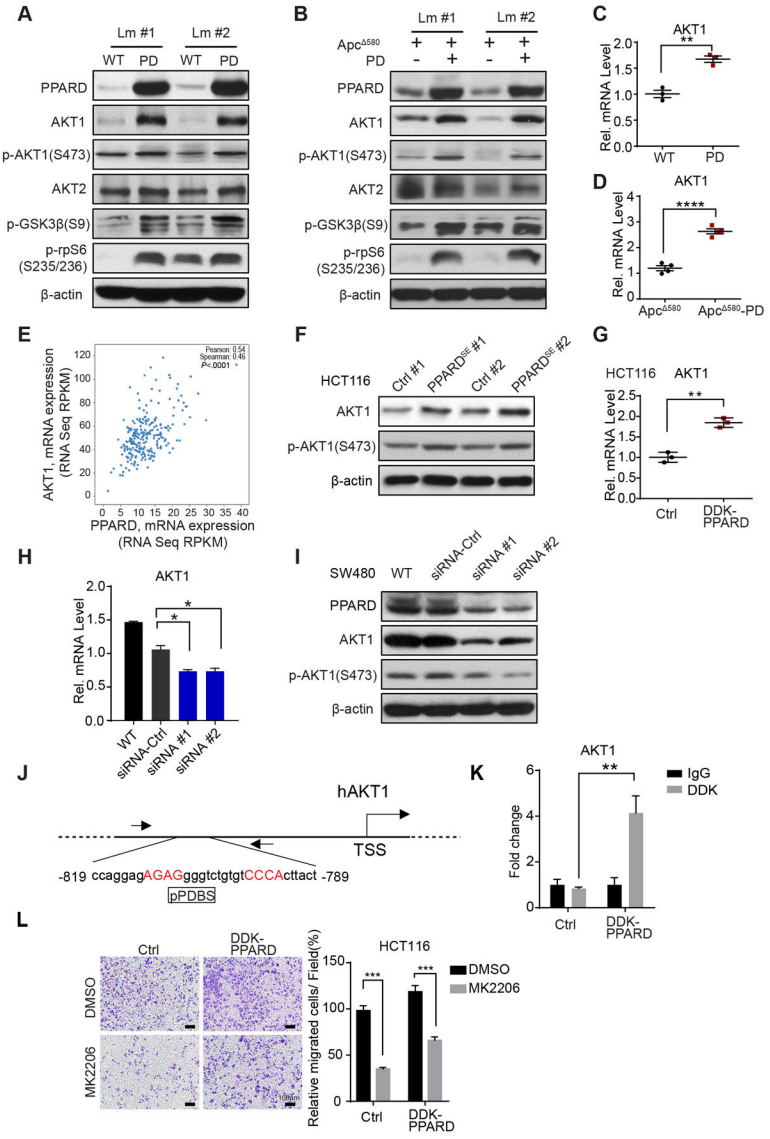


**Figure 6.**

PPARD transcriptionally activates the AKT1/p-rpS6 pathway in IECs. **A and B,** Effects of PPARD on the AKT1 signaling pathway in IECs in the mice. Protein expression levels of AKT1, p-AKT1 (S473), AKT2, p-GSK3β, and p-rpS6 (S235/236) in IECs of PD mice (**A**), Apc$^{\Delta 580}$-PD mice (**B**), and their corresponding control littermates (Lm). **C and D,** AKT1 mRNA expression levels in PD (**C**) and Apc$^{\Delta 580}$-PD mice (**D**) and their control littermate mice. **E,** Correlation analysis of PPARD and AKT1 mRNA expression in the TCGA colorectal adenocarcinoma database (Nature, 2012) database (n = 244). **F,** Protein expression levels of AKT1 and p-AKT1 (S473) in HCT116 cells stably transfected with a PPARD expression plasmid (PPARD$^{SE}$) or a control (Ctrl) plasmid. #: clone number. **G,** AKT1 mRNA levels in the HCT116 cells stably transduced with DDK-PPARD or control (Ctrl) lentiviral particles. **H,** AKT1 mRNA levels in SW480 cells transfected with 2 independent PPARD siRNAs or a control siRNA. **I,** AKT1 and p-AKT1(S473) protein expression levels in the SW480 cells transfected with PPARD siRNAs described in panel H. **J,** Schematic map

of the potential PPARD binding site (pPDBS) in the promoter region of human AKT1 (hAKT1) according to Genomatix MatInspector online software. Nucleotides in red indicate core sequences. TSS: transcription start site. **K,** PPARD binding to the pPDBS of the AKT1 promoter shown in panel J, measured by a chromatin immunoprecipitation-quantitative PCR assay in HCT116 cells used for panel G. **L,** Effects of AKT1 inhibition on PPARD promotion of colon cancer cell migration. Migration was assessed in HCT116-DDK-PPARD and HCT116-Ctrl cells as described in panel G, treated with an AKT inhibitor (MK2206) (1.0 μM) or vehicle solvent (DMSO) for 36 hours. **Left,** representative photomicrographs of migrated cells. **Right,** migrated cells in at least 4 random individual fields per insert membrane were counted. Data are mean ± SEM. *$P< 0.05$, **P < $0.01$, ***$P < 0.001$, and ****$P < 0.0001$.

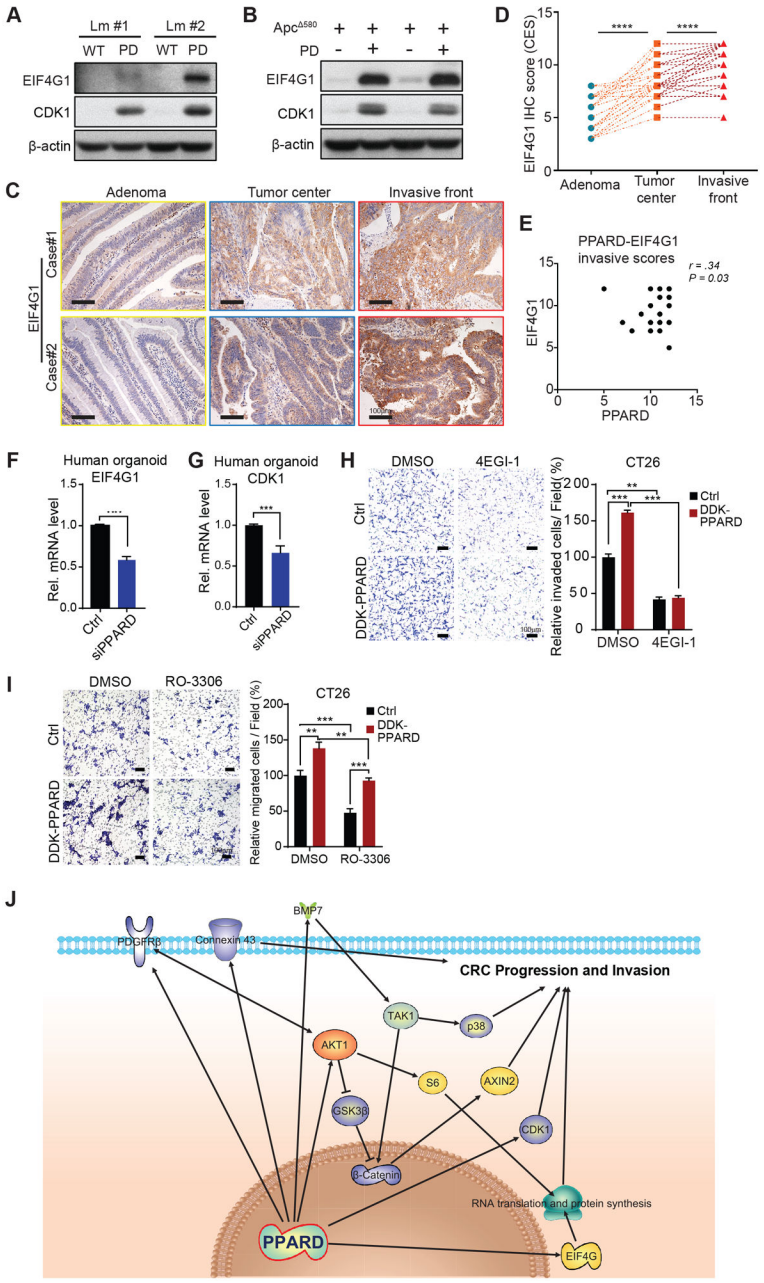


**Figure 7.**

PPARD upregulates EIF4G1 and CDK1 expression in IECs. **A and B,** EIF4G1 and CDK1 protein expression levels in IECs from PD (**A**) and $Apc^{\Delta 580}$-PD (**B**) mice and their corresponding control littermates. **C-E,** EIF4G1 expression in human colorectal cancer invasive fronts. **C,** Representative EIF4G1 IHC staining images of human paired colorectal adenomas, CRC tumor centers, and CRC invasive fronts of 2 patients. **D,** Total combined CES of nucleus and cytoplasm IHC staining of EIF4G1 for the paired colorectal adenomas, CRC tumor centers, and CRC invasive fronts (n = 41 patients). **E,** Correlation analysis of PPARD and EIF4G1 IHC scores for invasive fronts from 41 patients. **F,** EIF4G1 mRNA expression level in human CRC organoid cells transfected with Ctrl-siRNA or PPARD

siRNA for 48 hours. PPARD downregulation by siRNA decreased EIF4G1 mRNA expression in human CRC organoid cells. **G,** PPARD downregulation by siRNA decreased CDK1 mRNA expression in human CRC organoid cells as described in panel F. **H,** Effects of EIF4G1 inhibitor 4EGI-1 on PPARD promotion of CT26 mouse colon cancer cell invasion. CT26 cells stably transduced with a control (Ctrl) or mouse DDK-PPARD lentiviral particles were treated with 4EGI-1 (50μM) or vehicle solvent (DMSO) for 48 hours. **Left:** representative photomicrographs of invaded cells. **Right:** invaded cells in at least 4 random individual fields per insert membrane were counted. **I,** Effects of CDK1 inhibitor RO-3306 on PPARD promotion of colon cancer cell migration. CT26 mouse colon cancer cells stably transduced with control (Ctrl) or DDK-PPARD lentiviral particles were treated with RO3306 (8.0 μM) or vehicle solvent (DMSO) for 36 hours. **Left:** representative photomicrographs of migrated cells. **Right:** migrated cells in at least 4 random individual fields per insert membrane were counted. **J,** Conceptual scheme of pro-invasive pathways that are upregulated by PPARD to promote CRC progression and invasion. Data are shown as mean ± SEM. $*P < 0.05$, $**P < 0.01$, $***P < 0.001$, and $****P < 0.001$.